

Synthesis and Thermoluminescence Studies of Dy³⁺ Doped Bi₂O₃ Nanophosphors

S. Ashwini^{1*}, K N Narasimhamurthy^{2*}

¹Department of Physics, Akshaya Institute of Technology, Tumkur-572106, India.

²Department of Physics, Government First Grade College, Tumkur, 572102, India.

Corresponding Author Orcid ID: 0000-0001-8180-207X

ABSTRACT

Detailed Thermoluminescence studies of Bi₂O₃ doped with Dy³⁺ synthesized by solution combustion method and irradiated with α -rays and β -rays for doses in the range from a few Gy to KGy was done in the current work. Powder X-ray diffraction (PXRD) analysis is used to calculate the average particle size and was determined to be in the range 13-30 nm. Thermoluminescence (TL) characteristics of β -rayed Bi₂O₃: Dy³⁺ doped samples for dose of 1 Gy to 20 Gy are studied. In all α -irradiated Bi₂O₃ : Dy³⁺ doped samples, at ~145 °C (T_{g1}) and ~155 °C (T_{g2}) two significant and well resolved TL glow peaks were observed. Also, the TL intensity is found to increase with dopant concentration up to 5 mol % and then decreases due to quenching. The peak position of both the glow peaks (T_{g1} and T_{g2}) is almost stable for the complete dose range. The activation energy and frequency factors are found to be 0.79 eV and 1.75×10¹⁵ s⁻¹ respectively. These values are in very good agreement with those values calculated by peak shape methods and are found to be 0.73 eV and 1.70×10¹⁵ s⁻¹ respectively.

Keywords— Bi₂O₃:Dy³⁺; Thermoluminescence; Activation energy; Frequency factors

1. Introduction

Nanophosphors (NPs) doped with Lanthanide (Ln³⁺) ions have gained substantial interest owing to their potential applications in diverse fields ranging from solar cells [1], remote photo activation [2], display [3], bio- imaging [4], drug release [5], solid state lasers [6], and temperature sensors [7]. Besides, NPs should possess advanced physicochemical characteristics, such as low toxicity, high resistance to photo bleaching, high penetration depth, long lifetimes, as well as great anti- Stokes shifts[8]. The only nontoxic heavy metal that can easily be purified in large quantities is Bismuth [9].

The semiconductors such as Bi₂O₃, BiOX (X= Br, Cl, I), Bi₂MoO₆ and BiVO₄ have a high refractive index and exceptional properties for photoluminescence, visible light absorption, dielectric permittivity, large oxygen ion conductivity, photoconductivity, and, notable, for photocatalytic activity. [10-13].

Among these semiconductors, the semiconductor with significant optical and electronic properties is Bismuth oxide (Bi₂O₃). Because of these properties, Bi₂O₃ has become a vital material for various applications such as photocatalysts [14], gas sensors [15], fuel cells [16], and electronic components [17]. Bi₂O₃ has 5 polymorphic forms (α , β , γ , δ and ω) with varied structures and properties [18], among which monoclinic α and face-centered cubic δ are stable at room temperature and at high temperature respectively. Bi₂O₃ NPs can be synthesized by various methods viz., sol-gel approach, micro-emulsion, sonochemical, hydrothermal, surfactant thermal strategy, chemical vapour deposition, solution combustion, microwave irradiation and electro-spinning [19].

In the present work the synthesis of Bi_{2-x}O₃: Dy_x (x= 0.01 to 0.11) NPs via effortless low temperature solution combustion method is reported. In comparison with conventional methods used for synthesis, the solution combustion method is beneficial with respect to low temperature and consumption of less time which yields in a high degree of crystallinity and homogeneity. The

synthesised NP is characterized by PXRD. The effect of Dy³⁺ doping on the thermoluminescence properties was analysed in detail for their probable usage in display applications.

2. Experimental Methods or Methodology

2.1. Synthesis

For the low solution combustion method, analytical grade Bismuth nitrate (Bi (NO₃)₃·5H₂O: 99.99%, Sigma Aldrich Ltd.) as Oxidizer, Dysprosium nitrate (Dy (NO₃)₃·6H₂O: 99.99%, Sigma Aldrich Ltd) as dopant and Urea as fuel are used for the synthesis of Bi_{2-x}O₃: Dy_x (x= 0.01 to 0.11). The aqueous solution containing stoichiometric quantity of reactants are taken in a cylindrical Petri dish (300 ml), such that Oxidizer to Fuel ratio is 1 (O/F=1) and introduced into a pre heated muffle furnace at temperature of 400 ±10 °C. Nano powders are resulted by the thermal dehydration of the reaction mixture with the liberation of gaseous products. Finally, the nano powders were calcined at 600 °C for 3 h [20].

2.2. Characterization

PXRD using X-ray diffractometer (Shimadzu) (V-50 kV, I-20 mA, λ-1.541Å, scan rate of 2° min⁻¹) was used to determine the Crystal morphology of the synthesised NPs. Thermoluminescence glow curves of β- and α- rayed Bi₂O₃: Dy³⁺ doped samples are analysed using a TL setup consisting of a small kanthal heating strip, temperature programmer, photomultiplier tube (RCA931A), and a milli voltmeter (Rishcom 100) at a heating rate of 5°Cs⁻¹.

3. Results and Discussion

3.1. PXRD studies

Figure 1 shows the PXRD pattern of Bi₂O₃ NPs doped with Dy³⁺ (1-11 mol %). All the recorded peaks were indexed to the Cubic phase of Bi₂O₃ (JCPDS card No.52-1007, Space Group: Fm-3m (no.225)), signifying high purity and crystallinity of the synthesized NPs. Scherer’s formula was used to determine the average crystallite size (D) [21]

$$D = \frac{0.9\lambda}{\Delta 2\theta} \quad \text{--- (1)}$$

where ‘λ’; wavelength of X-rays, and ‘Δ2θ’; Full width half maxima (FWHM) of XRD peaks. D value of Bi₂O₃:Dy³⁺ (1-11 mol %) samples lies in the range 13-30 nm which indicates that, the value of D decreases with the increase of doping concentration, which is due to the fact that the addition of Dy³⁺ ions decreases the gap between conduction and valence bands.

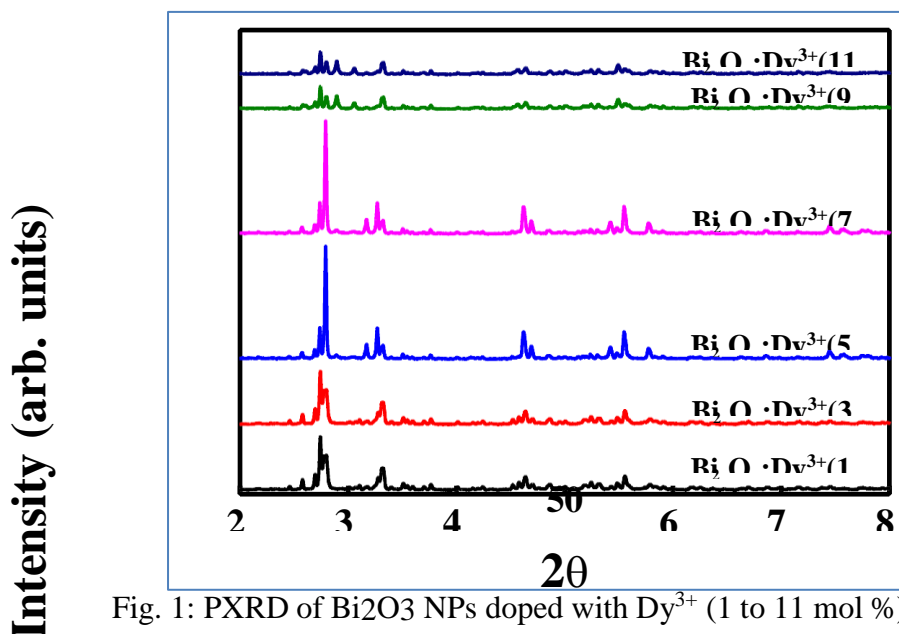


Fig. 1: PXRD of Bi₂O₃ NPs doped with Dy³⁺ (1 to 11 mol %)

3.2. Glow curves of Bi₂O₃: Dy³⁺ (5 mol %)

Figure 2 shows the TL glow curves of Bi₂O₃: Dy³⁺ (1-9 mol %) gamma rayed for dose 1 kGy. The glow curves clearly shows two prominent and well resolved glows with peaks at ~ 145 °C (T_{g1}) and

~ 155 °C (T_{g2}) along with a shoulder peak at ~ 163 °C. It also shows that TL intensity increases almost linearly with increase in gamma ray dose upto 5 mol % and then decreases for higher mol concentration of Dy. The decreases in intensity may be due to quenching. The peak position of TL glow for both T_{g1} and T_{g2} is almost stable for the complete dose range. The intensity of TL glow peak decreases at higher concentration of dopant ions and this might be probably due to the occupancy of deep traps and also due to disorganization of the initial energy levels. The variation of glow peak intensity and position as a function of concentration is shown in figure 3 [22, 23]. The kinetic parameters were determined according to glow curve shape method (modified by Chen) using CGCD as shown in Figure 4 and results are tabulated in Table 1. TL glow peak depends on a range of parameters such as history of the samples, heat-treatment of the samples preceding irradiation, physical nature of the sample, impurity content of the sample, nature and amount of dose given to the sample, temperature at which irradiation as well as TL measurements are made, environment of the sample while irradiation, rate of heating the sample etc.

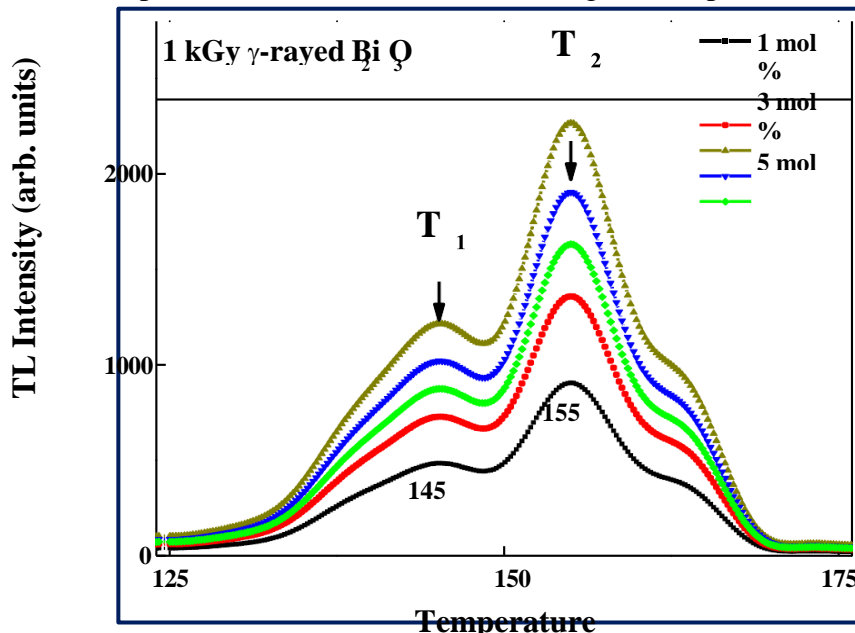


Fig 2. Thermoluminescence glow curves in γ -rayed Bi₂O₃ nanocrystals ($\beta=5^\circ\text{Cs}^{-1}$).

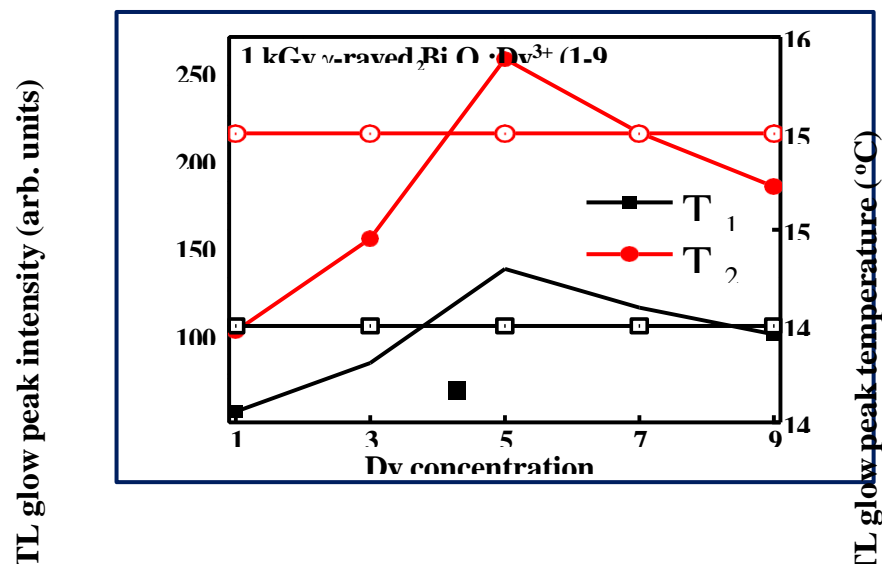




Fig 3. TL glow peak intensity and temperature as a function of dose

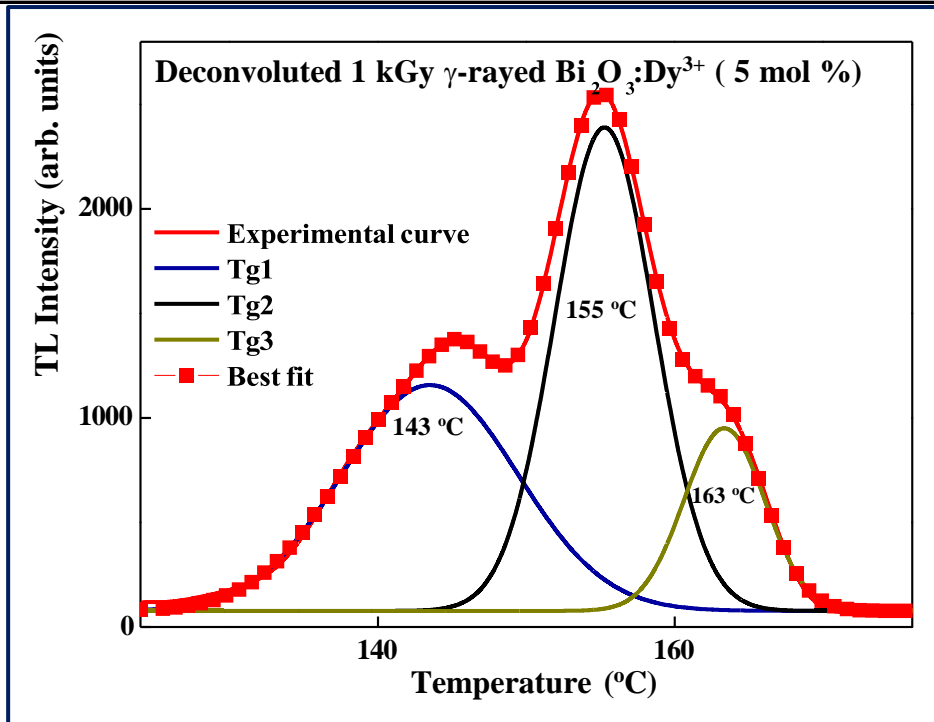


Fig 4. CGCD thermoluminescence glow curve γ -rayed $\text{Bi}_2\text{O}_3:\text{Dy}^{3+}$ (5 mol %)

Table 1. TL kinetic parameters of $\text{Bi}_2\text{O}_3:\text{Dy}^{3+}$ irradiated with γ -rays for 1 KGy obtained by the glow curve shape method (modified by Chen).

Glow Peak temperature, T_m (°C)	Glow peak parameters				TL parameters		
	δ (°C)	τ (°C)	ω (°C)	μ_g	E_t (eV)	n_0 (cm^{-3})	S (s^{-1})
143	7.05	7.1	14	0.5	0.929	980	8.42×10^{13}
155	4	3	7	0.45	0.73	1294	1.70×10^{15}
163	4	3	7	0.44	0.815	515	5.12×10^{16}

The influence of different heating rates from 5 °C/s to 40 °C/s on the TL response has been carried out for $\text{Bi}_2\text{O}_3:\text{Dy}^{3+}$ (5 mol %). It was found that as heating rate increases, the peak intensity and the total area of the main peak decreases whereas the peak temperature (T_m) moves towards higher temperature. This may be attributed to the thermal quenching of TL. Fig 5 shows TL glow curves of $\text{Bi}_2\text{O}_3:\text{Dy}^{3+}$ (5 mol %) γ -rayed for 1 kGy at different heating rates (β). It is seen that with the variation in heating rates, peak shape varies and there is a shift in the peak position. This can be explained as follows. At low heating rate the time spend by the phosphor is large enough so that certain quantity of thermal release of electrons depending on the half life at this temperature could take place. Now, as the heating rate increases the time spend at the same temperature decreases and hence the thermal release of electrons is also decreased. So, a much higher temperature is required for the same amount of thermal release to happen. In this manner the whole glow peak is shifted to higher temperature as the heating rate increases in a way depending on the half life and the time spent at each temperature [24].

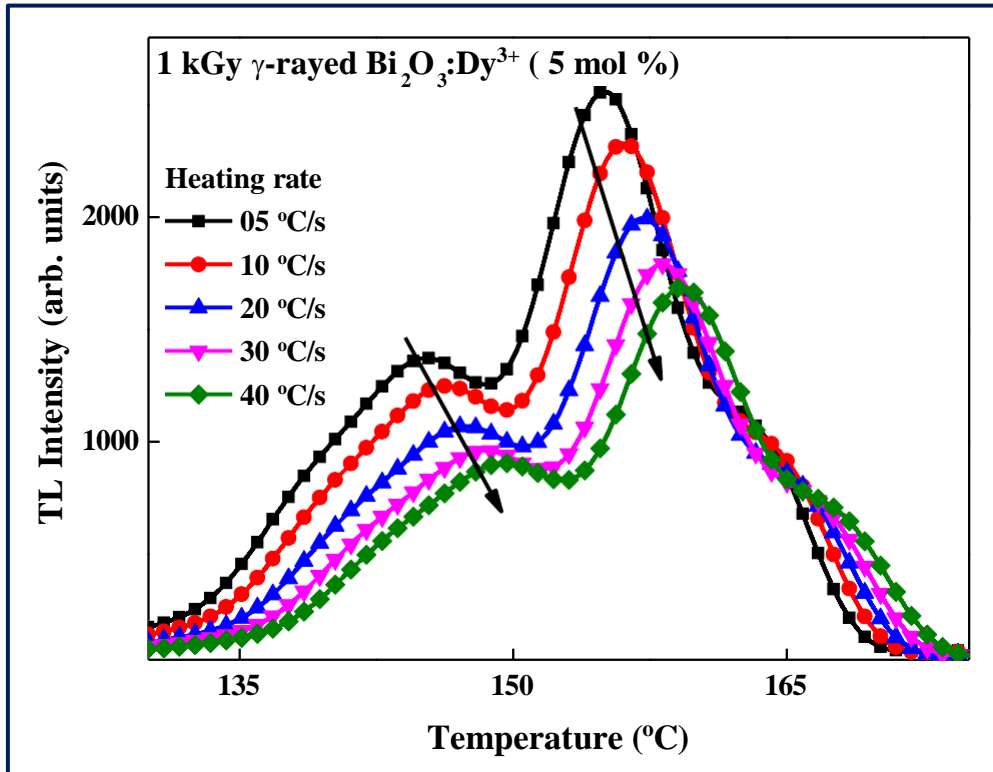


Fig 5 Thermoluminescence glow curves of Bi₂O₃: Dy³⁺ (5 mol %) γ-rayed for 1 kGy at different heating rates (β)

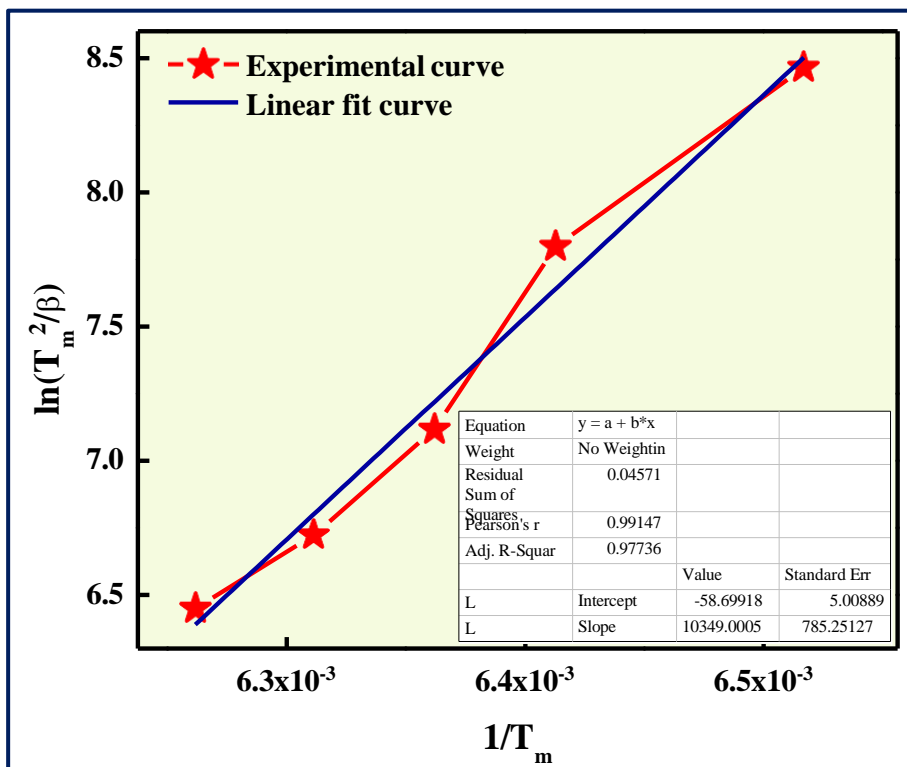


Fig 6. Variation of $\ln(T_m^2/\beta)$ v/s $1/T_m$ in TL glow curves of Bi O : Dy³⁺ (5 mol %) γ-rayed for 2 mm² 3 kGy at different heating rates (β)

The variable heating rate (VHR) method is used to find the trapping parameters as given by Chen et al and Yazici et al [25,26]. According to them a $\ln(T_m^2/\beta)$ against $1/T_m$ gives a straight line with slope equal to E/k , where 'k' is the Boltzmann constant, 'E' trap depth. Extrapolation of straight line to $1/T_m = 0$ gives a value of $(s k/E)$ from which the frequency factor 's' can be found by insertion of E/k found from the slope. Figure 6 shows the plot of variation of $\ln(T_m^2/\beta)$ v/s $1/T_m$ in TL glow curves of $\text{Bi}_2\text{O}_3:\text{Dy}^{3+}$ (5 mol %) γ -rayed for 1 kGy at different heating rates (β). From the plot, the activation energy and frequency factors are found to be 0.79 eV and $1.75 \times 10^{15} \text{ s}^{-1}$ respectively. These values are in very good agreement with those values calculated by peak shape methods where the activation energy and frequency factors are found to be 0.73 eV and $1.70 \times 10^{15} \text{ s}^{-1}$.

The behaviour of FWHM is an outcome of the whole glow peak shift versus heating rate since it is measured as a temperature difference within the glow peak region. Thus it is precisely same as that of T_{max} . Similar results were observed by Gorbics et. al [27] where a decrease of both integral and peak height happens and the glow peak shifts to higher temperatures due to thermal quenching. Taylor and Lilley [28] experimented a reduction in TL intensity of LiF at high heating rates.

The phenomenon of the decrease in the TL intensity with heating rate is a universal one. This was observed in various materials and is independent of the nature of specific impurity. For all these observations, the back ground under each glow peak was kept zero for all heating rate, i.e., the thermal release of trapping species is complete. Hence we can assign the decrease in TL intensity to the recombination process, i.e., trapping species in the conduction band and luminescence centers. As carrier pile up is lined out at these heating rates, the reduction in the normalized TL is due to thermal quenching of the luminescence centers. The increase in the glow peak temperature with increase of heating rate for recording the TL signal is a universal phenomenon [29,30].

CONCLUSION

Detailed Thermoluminescence studies of Bi_2O_3 doped with Dy^{3+} and Sm^{3+} synthesized by solution combustion method and irradiated with α -rays and β -rays for doses in the range from a few Gy to KGy was done in this chapter. In all α -irradiated $\text{Bi}_2\text{O}_3:\text{Dy}^{3+}$ doped samples, two prominent and well resolved TL glow peaks at $\sim 145^\circ\text{C}$ (T_{g1}) and $\sim 155^\circ\text{C}$ (T_{g2}) are observed. Also, the TL intensity is found to increase with dopant concentration up to 5 mol % and then decreases due to quenching. The peak position of both the glow peaks (T_{g1} and T_{g2}) is almost stable for the complete dose range. The increase in TL glow peak intensity initially may be due to the occupancy of deep traps and it may be attributed to disorganization of the initial energy levels as a result of high dose.

References

1. J. de Wild, A. Meijerink, J. K. Rath, W. G. J. H. M. van Sark and R. E. I. Schropp, "Upconverter solar cells: materials and applications", *Energy Environ. Sci.*, 4 (2011) 4835.
2. Jayakumar MK, Idris NM, Zhang Y, "Remote activation of biomolecules in deep tissues using near-infrared-to-UV upconversion nanotransducers", *Proc. Natl. Acad. Sci. U S A.* 109 (2012) 8483-8.
3. R. Deng, F. Qin, R. Chen, W. Huang, M. Hong and X. Liu, "Temporal full-colour tuning through non-steady-state upconversion", *Nat. Nanotechnol.*, 10 (2015) 237.
4. Jing Zhou, Zhuang Liu and Fuyou Li, "Upconversion nanophosphors for small-animal imaging", *Chem. Soc. Rev.*, 41 (2012) 1323–1349.
5. Shen J, Zhao L, Han G, "Lanthanide-doped upconverting luminescent nanoparticle platforms for optical imaging-guided drug delivery and therapy", *Adv. Drug Deliv. Rev.*, 65 (2013)744- 55
6. G. Rumbles, "Synthesis and upconversion luminescence of $\text{BaY}_2\text{F}_8:\text{Yb}^{3+}/\text{Er}^{3+}$ nanobelts", *Nature*, 409 (2001) 572-573.
7. Fischer LH, Harms GS, Wolfbeis OS, "Upconverting nanoparticles for nanoscale thermometry",

Angew Chem Int Ed Engl. 50 (2011) 4546-51

8. [Huang P](#), [Zheng W](#), [Zhou S](#), [Tu D](#), [Chen Z](#), [Zhu H](#), [Li R](#), [Ma E](#), [Huang M](#), [Chen X](#), “Lanthanide-doped LiLuF(4) upconversion nanoprobles for the detection of disease biomarkers”, [Angew. Chem. Int. Ed. Engl.](#), 53 (2014)1252-7.

9. P. Lei, X. Liu, L. Dong, Z. Wang, S. Song, X. Xu, Y. Su, J. Feng and H. Zhang, “Lanthanide doped Bi₂O₃ upconversion luminescence nanospheres for temperature sensing and optical imaging”, *Dalton Trans.*, 2015, DOI: 10.1039/C5DT04279H.

10. Aijuan Han, Jiulong Sun, Gaik Khuan Chuah and Stephan Jaenicke, “Enhanced *p*-cresol photodegradation over BiOBr/Bi₂O₃ in the presence of rhodamine B”, *RSC Adv.*, 2017, 7, 145- 152.

11. Tamar Saison, Nicolas Chemin, Corinne Chaneac, Olivier Durupthy, Valerie Ruauux, Laurence Mariey, Francoise Mauge, Patricia Beaunier, and Jean-Pierre Jolivet, “Bi₂O₃, BiVO₄, and Bi₂WO₆: Impact of Surface Properties on Photocatalytic Activity under Visible Light”, *The Journal of Physical Chemistry C*, 2011, 115, 5657–5666.

12. K. Li, Y. Tang, Y. Xu, Y. Wang, Y. Huo, H. Li, J. Jia, “A BiOCl film synthesis from Bi₂O₃ film and its UV and visible light photocatalytic activity”, *Applied Catalysis B, Environmental* (2013), <http://dx.doi.org/10.1016/j.apcatb.2013.04.005>.

13. Xiaochao Zhang, Tianyu Guo, Xiaowen Wang, Yawen Wang, Caimei Fan, Hui Zhang, “Facile composition-controlled preparation and photocatalytic application of BiOCl/Bi₂O₂CO₃ nanosheets”, *Applied Catalysis B: Environmental* 150– 151 (2014) 486–495.

14. Hassan Najafiana, Faranak Manteghia, Farshad Beshkarb, Masoud Salavati-Niasaric, “Enhanced photocatalytic activity of a novel NiO/Bi₂O₃/Bi₃ClO₄ nanocomposite for the degradation of azo dye pollutants under visible light irradiation”, *Separation and Purification Technology*, 209 (2019) 6–17.

15. H. Takeda, T. Ueda, K. Kamada, K. Matsuo, T. Hyodo, Y. Shimizu, “CO-sensing properties of a NASICON-based gas sensor attached with Pt mixed with Bi₂O₃ as a sensing electrode”, *Electrochim. Acta*, 155 (2015) 8-15.

16. W. zuo, W. Zhu, D. Zhao, Y. Sun, Y. Li, J. Liu and X. W. D. Lou, “Bismuth oxide: a versatile high-capacity electrode material for rechargeable aqueous metal-ion batteries”, *Energy Environ. Sci.*, 9 (2016) 2881.

17. L. Li, X. Zhang, Z. Zhang, M. Zhang, L. Cong, Y. Pan, S. Lin, *J. Mater. Chem. A* 2016, 4, 16635.

18. Yanlin Huang , Jie Qin, Xuanxuan Liu , Donglei Wei, Hyo Jin Seo, “Hydrothermal synthesis of flower-like Na-doped α -Bi₂O₃ and improved photocatalytic activity via the induced oxygen vacancies”, *Journal of the Taiwan Institute of Chemical Engineers*, <https://doi.org/10.1016/j.jtice.2018.11.029>.

19. Ashwini S, Prashantha SC, Naik R, Nagabhushana H, “Enhancement of luminescence intensity and spectroscopic analysis of Eu³⁺ activated and Li⁺ charge-compensated Bi₂O₃ nanophosphors for solid-state lighting”, *Journal of Rare Earths*, Volume 37, Issue 4, April 2019, Pages 356-364. <https://doi.org/10.1016/j.jre.2018.07.009>

20. S. Ashwini, S.C. Prashantha, Ramachandra Naik, H. Nagabhushana, D.M. Jnaneshwara, K.N. Narasimhamurthy, “Bi₂O₃:Dy³⁺ nanophosphors: its white light emission and photocatalytic activity”, *SN Applied Sciences*, 1(9) (2019) 1028. <https://doi.org/10.1007/s42452-019-1047-6>

21. P. Klug, L. E. Alexander, “X-Ray Diffraction Procedure”, Wiley, New York, 1954.

22. E. Yukihiro, R. Gaza, S. McKeever, C. Soares, “Optically stimulated luminescence and thermoluminescence efficiencies for high-energy heavy charged particle irradiation in Al₂O₃: C”, *Radiation measurements*, 38 (2004) 59-70.

23. N. Salah, P. Sahare, “The influence of high-energy ⁷Li ions on the TL response and glow curve structure of CaSO₄: Dy”, *Journal of Physics D: Applied Physics*, 39 (2006) 2684.

24. G. Kitis, M. Spiropulu, J. Papadopoulos, S. Charalambous, “Heating rate effects on the TL



glow-peaks of three thermoluminescent phosphors”, Nuclear Instruments and Methods in Physics Research Section B: Beam Interactions with Materials and Atoms, 73 (1993) 367- 372.

25. R. Chen, S. Winer, “Effects of various heating rates on glow curves”, Journal of Applied Physics, 41 (1970) 5227-5232.

26. A.N. Yazici, M. Öztaş, V.E. Kafadar, M. Bedir, H. Toktamış, “The analysis of thermoluminescent glow peaks of copper doped ZnS thin films after β -irradiation”, Journal of luminescence, 124 (2007) 58-66.

27. S.G. Gorbics, A.E. Nash and F.H. Attix, in: Proc. 2nd Int.Conf.on Lumin. Dosimetry. T.N. Gattinberg, USA, p. 587 (1968)

28. G. Taylor, E. Lilley, “Rapid readout rate of studies of thermoluminescence in LiF (TLD-100) crystals”, Journal of Physics D: Applied Physics, 15 (1982) 2053.

29. A. Pradhan, “Influence of heating rate on the TL response of LiF TLD-700, LiF: Mg, Cu, P and Al₂O₃: C”, Radiation protection dosimetry, 58 (1995) 205-209.

30. A. Pradhan, “Thermal Quenching and Two Peak Method-Influence of Heating Rates in TLDs”, Radiation protection dosimetry, 65 (1996) 73-78.